NeuroImage 52 (2010) 1080–1094

Contents lists available at ScienceDirect

NeuroImage

journal homepage: www.elsevier.com/locate/ynimg

The generation of rhythms within a cortical region: Analysis of a neural mass model

Mauro Ursino *, Filippo Cona, Melissa Zavaglia

Department of Electronics, Computer Science and Systems, University of Bologna, Bologna, Italy

ARTICLE INFO

Article history:
Received 28 July 2009
Revised 18 December 2009
Accepted 21 December 2009
Available online 4 January 2010

Keywords:
EEG rhythms
Connectivity
Neural mass models
$GABA_{A,fast}$ inhibitory interneurons
Power spectral density

ABSTRACT

Rhythms in brain electrical activity are assumed to play a significant role in many cognitive and perceptual processes. It is thus of great value to analyze these rhythms and their mutual relationships in large scale models of cortical regions. In the present work, we modified the neural mass model by Wendling et al. (Eur. J. Neurosci. 15 (2002) 1499–1508) by including a new inhibitory self-loop among $GABA_{A,fast}$ interneurons. A theoretical analysis was performed to demonstrate that, thanks to this loop, $GABA_{A,fast}$ interneurons can produce a γ rhythm in the power spectral density (PSD) even without the participation of the other neural populations. Then, the model of a whole cortical region, built upon four interconnected neural populations (pyramidal cells, excitatory, $GABA_{A,slow}$ and $GABA_{A,fast}$ interneurons) was investigated by changing the internal connectivity parameters. Results show that different rhythm combinations (β and γ, α and γ, or a wide spectrum) can be obtained within the same region by simply altering connectivity values, without the need to change synaptic kinetics. Finally, two or three cortical regions were connected by using different topologies of long range connections. Results show that long-range connections directed from pyramidal neurons to $GABA_{A,fast}$ interneurons are the most efficient to transmit rhythms from one region to another. In this way, PSD with three or four peaks can be obtained using simple connectivity patterns. The model can be of value to gain a deeper insight into the mechanisms involved in the generation of γ rhythms and provide a better understanding of cortical EEG spectra.

Introduction

Analysis of brain activity at a mesoscopic scale (from a millimeter to several centimeters of the cortex) reveals the presence of synchronous oscillations, which cover a large spectrum of frequencies and can be detected using EEG, MEG or ECoG (Buzsàki, 2006). It is generally assumed that these oscillations are not merely an epiphenomenon, but play a crucial role in many important processes of the cortex, especially involving association among different functions (Basar et al., 2000, 2001; Ward, 2003). The study of brain rhythms, in turn, of their etiology and functional role is strictly connected with the estimation of effective connectivity among brain regions. Rhythms originating in one region, in fact, may be transmitted to other regions via long range excitatory connections, and this "system of rhythms" may serve important functions to associate information from one region to another, to detect the phase of events, or to drive synaptic plasticity, thus playing a pivotal role in learning and memory (Basar et al., 2000, 2001; Engel and Singer, 2001; Ward, 2003).

One way to improve our knowledge of this "system of rhythms," and to investigate the correlated problem of effective cortical connectivity, is through the use of dynamical mathematical models. In particular, a discipline named neurodynamics aims at analyzing the operations of the brain by investigating (via mathematical models and signal processing techniques) the dynamical aspects of electric or magnetic brain activity (Freeman, 1975; Nunez, 1995).

Mathematical models used to study brain dynamics can be roughly subdivided into two main classes, each with its virtues and drawbacks. In a first class of models, the activity of individual neurons is described in detail (generally using spiking neurons) and the properties of ionic channels, axons and dendrites often incorporated explicitly (Maex and De, 2007; Traub et al., 2005; Wang and Buzsaki, 1996). Although these models are of the greatest value to understand the basic mechanisms of neural dynamics at a microscopic scale (for instance, to investigate mechanisms causing oscillations in a network of neurons), they are too cumbersome and computationally onerous to analyze the behavior of entire cortical regions at a mesoscopic level.

Much attention in recent years has been devoted to the so-called "neural mass models" (NMMs), first introduced by Wilson and Cowan (1972), Freeman (Freeman, 1978), and Lopes da Silva et al. (1974) in the mid-seventies. In these models, the dynamics of entire neural populations and of their synapses are described using just a few state variables (i.e., a few differential equations) under the assumption that neurons in the same population share similar inputs and synchronize their activity. Besides a smaller computational complexity, these models offer a more parsimonious description of neural dynamics in terms of parameters and mechanisms involved, generally ascribing

* Corresponding author. Dipartimento di Elettronica, Informatica e Sistemistica, viale Risorgimento 2, I-40136 Bologna, Italy. Fax: +39 051 2093073.
E-mail address: mauro.ursino@unibo.it (M. Ursino).

1053-8119/$ – see front matter © 2009 Elsevier Inc. All rights reserved.
doi:10.1016/j.neuroimage.2009.12.084

rhythm generation to feedback loops between excitatory and inhibitory neural populations. One of the first models of this type is the Wilson-Cowan oscillator, which is still largely used today to study synchronization among neural oscillations (Wilson and Cowan, 1972). Lopes da Silva et al. (1974) proposed a simple model of two populations in feedback (one excitatory and the other inhibitory) to simulate the generation of the α rhythm in the thalamus. Freeman proposed a similar model to study dynamics in the olfactory cortex (Freeman, 1978). These models have been subsequently improved by Jansen et al. (1993) and Jansen and Rit (1995): their model encompasses the interaction between three neural populations with different synaptic kinetics (pyramidal neurons, excitatory interneurons, inhibitory interneurons), as it occurs in a single cortical column. The Jansen equations are frequently used today to build models of interconnected cortical areas devoted to the analysis of EEG dynamics in large regions of the brain (David and Friston, 2003), to study effective connectivity from EEG or fMRI data (Babajani and Soltanian-Zadeh, 2006) or to investigate how event related potentials (ERPs) depend on intrinsic connectivity (David et al., 2005). The group of Friston (Friston, 2005; Kiebel et al., 2008) developed a mathematical formalism, named Dynamic Causal Modeling (DCM), to provide a theoretical framework for the study of brain dynamics: it uses some variations of the Jansen model to characterize dynamics in cortical regions, together with a Bayesian approach for parameter estimation from data. Others (Babajani and Soltanian-Zadeh, 2006) used neural mass models to link data obtained from metabolic imaging (PET or fMRI) and electromagnetic signals (EEG or MEG). Sotero et al. (2007) developed a model of the overall cortical dynamics (still based on a variation of the Jansen model) to investigate how the distribution of brain rhythms on the cortex may depend on effective connectivity among the ROIs (regions of interest). Their model includes 71 brain areas with anatomical connectivity matrices among these areas. Models for the analysis of EEG at a mesoscopic scale were formulated by Wright, Robinson, and Rowe et al. in a series of papers from the mid-nineties (Rennie et al., 2002; Robinson et al., 2001; Wright et al., 2003). Although these models use a continuum in space instead of discrete neural populations, they share many aspects with neural mass models; in particular they exploit a few equations to summarize neural dynamics.

An important advancement in the use of neural mass models was provided by Wendling et al. (2002). Studying hippocampal dynamics during epilepsy, they proposed the addition of a fourth population to the Jansen model to account for the presence of $GABA_A$ interneurons with fast synaptic kinetics (White et al., 2000). With this model, they were able to simulate the dynamics of real EEG signals measured with intracerebral electrodes in the hippocampus during the transition from interictal to fast ictal activity. Recently, the Wendling model was used by Ursino and Zavaglia et al. to simulate the multimodal power spectral density in cortical regions (Zavaglia et al., 2006, 2008) and to assess cortical connectivity via parameter estimation techniques (Cona et al., 2009; Ursino et al., 2007) during simple motor tasks. In particular, these studies stress the importance of fast inhibitory interneurons in the genesis of power in the γ band.

Neural mass models were used by Moran et al. (2007, 2009) in a series of recent papers to simulate spectral densities of EEG and MEG recordings. In these last models, the authors introduced recurrent connections among inhibitory interneurons and spike rate adaptation. Using linearity and stationarity assumptions, they investigated how the model's biophysical parameters (e.g., post-synaptic receptor density and time constants) influence the cross-spectral density of responses measured directly.

This short summary underlines the rising importance that neural mass models are acquiring for the study of brain dynamics. Analysis of the literature, however, and previous simulations of our group (Ursino et al., 2007; Zavaglia et al., 2006) also reveal some important limitations of these models. First, a single neural mass model (consisting of three (Jansen) or four (Wendling) neural populations connected via multiple feedbacks) when stimulated with input white noise produces just a single rhythm, with a narrow band, or, in some cases, a wide band spectrum. This "intrinsic rhythm" may originate either from instability of the feedback loops or, more frequently, from noise amplification caused by a resonance in a given frequency band (Grimbert and Faugeras, 2006). Moreover, to produce rhythms in different bands, these models necessitate a change in the synaptic time constants. In particular, simulating γ rhythms in these models requires the use of very small values for the time constant of fast interneurons (i.e., a few ms) (Wendling et al., 2002; Zavaglia et al., 2008). Conversely, real spectra measured during motor or cognitive tasks often reveal the presence of multiple rhythms in the same ROI (Rowe et al., 2004; Ursino et al., 2007; Zavaglia et al., 2006). The simultaneous coexistence of several rhythms appears as an important characteristic of brain dynamics, which may have important computational functions.

Hence, the following problems are "on the table." How can we simulate different rhythms in a single ROI within the framework of NMMs? Are these models adequate to simulate γ oscillations, which play an essential role in many high-level cognitive tasks?

David and Friston (2003) suggested that a multi-modal spectrum can be obtained via NMMs by assuming the presence of different sub-populations in the same cortical region with different synaptic kinetics (i.e., different sub-populations of pyramidal neurons, excitatory interneurons, etc…). A similar approach was followed by Ursino et al. (2007) and Zavaglia et al. (2006) to simulate α, β and γ rhythms in some ROIs during simple motor tasks. It is worth noting that the same idea was implicitly followed also by Sotero et al. (2007); in fact, these authors simulated the distribution of δ, α, β and γ rhythms separately, which is the same as to consider four separate systems of rhythms with distinct sub-populations of neurons. Although this approach may be consistent with the physiological reality, it appears not parsimonious: you need one specific population of neurons for each rhythm you want to generate. A more parsimonious approach was proposed by our group recently: we hypothesized that each region can produce just one intrinsic rhythm due to its internal dynamics, but it can receive additional rhythms from other regions via long-range excitatory connections (Cona et al., 2009; Zavaglia et al., 2008). With this model, one does not need to replicate too many populations of neurons, but still needs to modify synaptic kinetics from one region to another. However, with this model, it is still difficult to obtain more than two simultaneous rhythms in the same ROI.

In the present work, we suggest a variation in NMMs which can help to overcome the previous limitations, and can be of value to build a system of interconnected rhythms among ROIs. Our variation is based on some recent experimental and modeling results, suggesting that γ rhythms can be generated by a network of fast inhibitory interneurons without the participation of the other populations.

Whittington, Traub and Jefferys (Jefferys et al., 1996; Whittington et al., 1995) numerically simulated a network of isolated inhibitory neurons tonically excited by an external input, and showed that the neurons tend to entrain their activity into rhythmic firing at about 40 Hz thanks to reciprocal inhibition. Subsequent studies which investigated the oscillatory behavior of large inhibitory interneuron networks assuming slow and weak synapses (Tiesinga and Jose, 2000; Wang and Buzsaki, 1996; White et al., 1998) confirmed that these networks can produce coherent oscillations when subject to external excitation. Oscillations, however, appeared scarcely robust to variations in the excitatory drive. To improve robustness, one needs to incorporate fast and strong inhibitory synapses into the network, but in this case a stronger external excitatory drive is required to overcome inhibition (Neltner et al., 2000). These results suggest that fast-spiking inhibitory interneurons play a pivotal role in the generation of γ-band oscillations (Bartos et al., 2007).

The previous modeling results are supported by experimental data. First, oscillations of inhibitory post-synaptic potentials at frequencies in the γ-band occur in the hippocampal and neocortical slices even after blockade of glutamate receptors (Jefferys et al., 1996; Whittington et al., 1995). Basket cells are highly interconnected in the hippocampus and in the neocortex (Bartos et al., 2007) where they can form an extensive mutually interconnected interneuron network (Kisvarday et al., 1993; Sik et al., 1995) with a large divergent synaptic output to other neurons (Cobb et al., 1995).

Despite the large number of theoretical and experimental data that stress the role of a fast inhibitory network in the genesis of γ-rhythms, we are not aware that this mechanism is solidly incorporated into neural mass models. Moran et al. incorporated recurrent self-connections between inhibitory interneurons in their recent model (Moran et al., 2007, 2008) motivating this choice with the necessity to generate high-frequency oscillations in the γ band. However, they used only one populations of inhibitory interneurons, without a distinction between $GABA_{A,fast}$ and $GABA_{A,slow}$ synaptic kinetics.

According to the previous discussion, three main objectives have been pursued in this work: (i) to enrich the NMM of a single region by adding a new feedback loop, through which fast inhibitory interneurons can produce a γ rhythm per se (i.e., without the participation of the other neural populations); (ii) to demonstrate that the modified model can easily produce EEG PSD of a single region characterized by two peaks (i.e., two activities in different bands), using a very parsimonious description of connectivity weights and without altering model time constants; and (iii) to demonstrate that a model of interconnected ROIs can produce complex multimodal spectra and that a long-range connection between two ROIs is much more efficient to transmit rhythms if it targets fast inhibitory interneurons, rather than pyramidal neurons.

The model is first presented in a synthetic form and the mechanism of γ-rhythm generation analyzed ("reduced model"). Then, the role of connectivity between populations of excitatory and inhibitory interneurons internal to the cortical region is studied, laying particular attention to the role of $GABA_{A,fast}$ interneurons ("complete model"). Subsequently, the effect of connectivity between two or three cortical regions is shown ("coupled complete model"). The discussion underlines the main innovative aspects of the proposed model.

Material and methods

A single region model: a brief summary

The model of a cortical region consists of four neural populations, which represent pyramidal neurons, excitatory interneurons, and inhibitory interneurons with slow and fast synaptic kinetics, respectively. Each population represents a group of neurons of the same type, which approximately share the same membrane potential and so can be lumped together. All populations are described with a similar mathematical formalism, as in Fig. 1.

Briefly, each population receives an average postsynaptic membrane potential (say v) from other neural populations, and converts this membrane potential into an average density of spikes fired by the neurons. In order to account for the presence of inhibition (when potential is below a given threshold) and saturation (when potential is high) this conversion is simulated with a static sigmoidal relationship. Moreover, each population sends synapses to other populations (or, in case of pyramidal neurons, to other regions too). Each synaptic kinetics is described with a second order system, but with different parameter values.

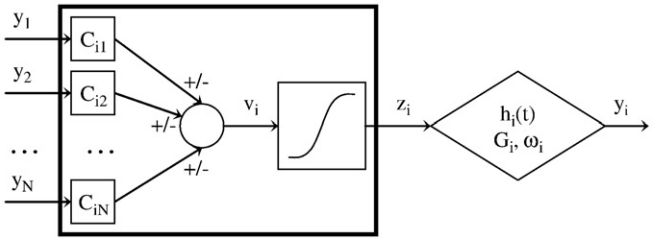

Fig. 1. Layout of the general model of a single population.

Throughout the present work, we will assume a *variational* model, i.e., all quantities are considered as variations with respect to a hypothetical basal value. Moreover, this basal value is taken at the central point of the sigmoidal relationship. As a consequence, all quantities have zero mean value and are centered at the basal value, assumed equal to zero. A similar assumption has been done also by others when developing recent neural mass models (David et al., 2005).

Of course, the use of a variational model also exhibits some important limitations: in particular, neither the position of the working point nor the slope of the sigmoid at the equilibrium value varies with the connectivity parameters. This simplification has been adopted to maintain the model in the linear region: this choice helps the analysis of rhythm transmission, avoiding that the equilibrium point in some population shifts to the sub-threshold or to the saturation region due to an excessive connectivity (see Ursino et al., 2007, for some exempla). This limitation can be overcome in future works, for instance by using a non-zero mean value for model inputs (thus making the equilibrium values to depend on connectivity parameters too).

In the following, a quantity which belongs to a neural population will be denoted with the subscript p (pyramidal), e (excitatory interneuron), s (slow inhibitory interneuron) and f (fast inhibitory interneuron).

Hence, the previous concepts are summarized by the following equations

$$v_i = \sum_j C_{ij} y_j \tag{2.1}$$

$$z_i = S(v_i) = \frac{2e_0}{1 + e^{-rv_i}} - e_0 \quad i=p,e,s,f \tag{2.2}$$

$$\ddot{y}_i = G_i \omega_i z_i - 2\omega_i \dot{y}_i - \omega_i^2 y_i \tag{2.3}$$

where the subscript j refers to a presynaptic neural population, y_j is the post-synaptic potential change induced by a unitary synapse, C_{ij} represent the connectivity constant from the jth population to the ith one, and the sum in the right hand member of Eq. (2.1) extends to all populations which make synapses to the ith population. Parameters e_0 and r in Eq. (2.1), assumed equal for all populations, set the maximal saturation and the slope of the sigmoidal relationship, while G_i and ω_i in Eq. (2.3) represent the strength and the reciprocal of the time constant of the individual synapses. It is worth noting that, by giving different values to G_i and ω_i ($i = p, e, s, f$) one can mimic the impulse responses of the different synapses (excitatory, $GABA_{A,slow}$ and $GABA_{A,fast}$). In the following, these impulse responses will be denoted with symbols $h_e(t)$, $h_s(t)$ and $h_f(t)$, assuming that excitatory interneurons have the same kinetics as pyramidal cells (i.e., $h_p(t) = h_e(t)$).

A network of fast inhibitory interneurons: the "reduced model"

Previous versions of neural mass models (Freeman, 1975; Jansen and Rit, 1995; Wendling et al., 2002) assumed that each neural population (p, e, s, f) receives its synaptic inputs from other populations in the same region or from pyramidal neurons in other regions. As a consequence, a neural population isolated from the others and stimulated by white noise cannot exhibit an intrinsic rhythm. Only connections with other populations can induce the

presence of rhythms, due to a balance between excitation and inhibition.

Conversely, experimental and computational results (summarized in the Introduction) underscore that a network composed of fast inhibitory interneurons can induce γ rhythms, even without the presence of other neural populations. Since this mechanism may play a significant role in the brain, providing a clock for pyramidal cells (Jefferys et al., 1996), we modified the description of the fast inhibitory interneurons taking into account the possible effect of their re-entrant connections. Indeed, basket cells (GABAergic interneurons) are highly interconnected and there is a high probability to find a chemical synapse between two closely placed fast-spiking basket cells (Bartos et al., 2007).

It is worth noting that the Jansen model was already modified in previous works with the introduction of a recurrent self-loop: for instance, Sotero et al. (2007) introduced a self-excitatory loop for the pyramidal population to account for the majority of intracortical fibers within a voxel; Moran et al. (2007) introduced a self-loop among inhibitory interneurons to generate γ rhythms. However, none of these models used $GABA_{A,fast}$ synapses.

The simple model of isolated fast inhibitory interneurons (named the "reduced model") is described in Fig. 2. Here, to have realistic dynamics, we assumed that these interneurons synapse with themselves (hence, we included a self-loop with impulse response $h_f(t)$) and are tonically excited by an external input (which may come from populations in the same area or from other cortical areas). The excitation is simulated with white noise (say $u_f(t)$) with zero mean value and variance $\sigma^2=5$, which acts through excitatory synapses (impulse response $h_e(t)$). The mean value of the input noise is taken as zero, since we are working with a variational model.

A deeper comprehension of the mechanisms through which this fast interneuron model generates a γ rhythm can be achieved via an analytical approach, by studying the linearized model around its critical points. The critical points are those for which the derivative of the state vector $Y_f=(y_f \dot{y}_f)$ is zero, at the mean value of the input ($u_f=0$). We can write:

$$\begin{cases} v_f = -C_{ff} y_f \\ z_f = S\left(v_f\right) = \dfrac{2e_0}{1+e^{-rv_f}} - e_0 \\ \dot{y}_f = 0 \\ \ddot{y}_f = G_f \omega_f z_f - 2\omega_f \dot{y}_f - \omega_f^2 y_f = 0 \end{cases} \tag{2.4}$$

where C_{ff} represents the strength of connections among inhibitory interneurons.

The only solution is the origin of the phase space $Y_f=(0,0)$, so $v_f=0$. The sigmoid is the only block that has to be linearized. By replacing its expression with the first order Taylor expansion in the critical point:

$$z_f = \left.\frac{\partial S\left(v_f\right)}{\partial v_f}\right|_{v_f=0} v_f = \frac{e_0 r}{2} v_f \tag{2.5}$$

one can obtain the transfer function of the linearized model in the frequency domain:

$$H(j\omega) = \frac{G_e \omega_e \left(\omega_f + j\omega\right)^2}{(\omega_e + j\omega)^2 \left[\omega_f\left(K+\omega_f\right) + 2\omega_f j\omega + (j\omega)^2\right]} \tag{2.6}$$

where $K = \frac{e_0 r}{2} C_{ff} G_f$ is the loop gain. It can be easily verified that if the parameters are all positive the model is asymptotically stable. H can be seen as the product of two transfer functions H_1 and H_2 such that

$$H_1(j\omega) = G_e \omega_e \frac{\left(\omega_f + j\omega\right)^2}{(\omega_e + j\omega)^2} \tag{2.7}$$

$$H_2(j\omega) = \frac{1}{\omega_f\left(K+\omega_f\right) + 2\omega_f j\omega + (j\omega)^2} \tag{2.8}$$

Since $\omega_e<\omega_f$, H_1 represents a low-pass filter which attenuates high-frequencies compared with the low frequencies (the attenuation ratio is $\omega_e<\omega_f$) and so it cannot be responsible for γ frequency amplification. H_2 is a second order low-pass filter, so its behavior is totally described by its natural frequency ω_n and its damping factor δ.

$$\omega_n = \sqrt{\omega_f\left(K+\omega_f\right)} \tag{2.9}$$

$$\delta = \sqrt{\frac{\omega_f}{K+\omega_f}} \tag{2.10}$$

If the parameters are chosen to have physiologically plausible values (see Results) then $\delta<\frac{1}{\sqrt{2}}$. In this case, a resonance occurs at ω_{peak}, where

$$\omega_{peak} = \sqrt{\omega_f\left(K-\omega_f\right)} \tag{2.11}$$

ω_{peak} is typically located in the γ band. The latter point will be examined in section results, via a parameters sensitivity analysis on K and ω_f.

Model of a single cortical area: the "complete model"

In the previous section, we considered only a single population, and so Eq. (2.11) holds only for the "reduced model." Of course, the activity of this gamma rhythm (and thus its frequency) changes when interneurons are connected to other populations. To model a whole cortical area (the "complete model," either an overall ROI as in Zavaglia et al. (2008), or a voxel as in Sotero et al. (2007)) we need to connect the four populations via excitatory and inhibitory synapses, with impulse response $h_e(t)$, $h_s(t)$ or $h_f(t)$. The average numbers of synaptic contacts among neural populations are represented by eight parameters, C_{ij} (see Fig. 3), where the first subscript represents the target (post-synaptic) population and the second subscript is the pre-

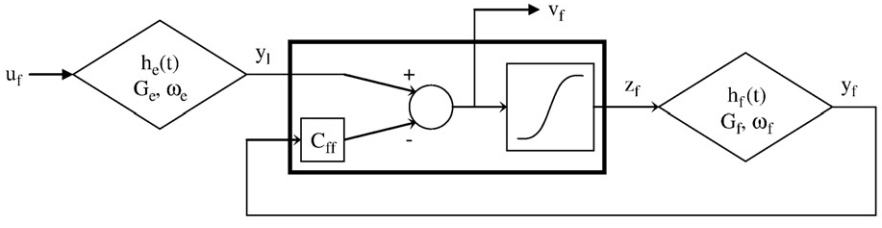

Fig. 2. Layout of the model of $GABA_{A,fast}$ inhibitory interneurons.

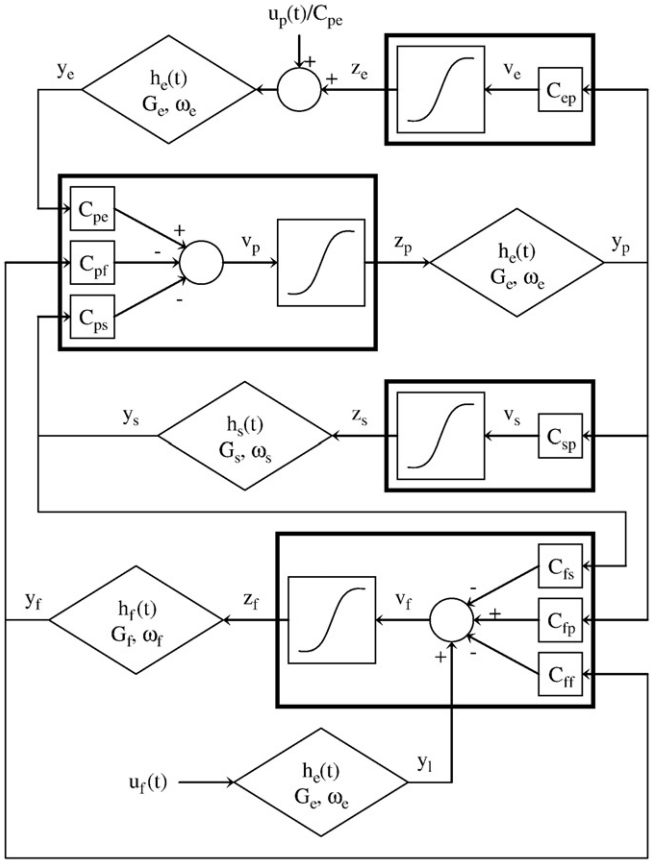

Fig. 3. Layout of the model of a single region: four neural populations (pyramidal cells, excitatory interneurons, $GABA_{A,slow}$ inhibitory interneurons and $GABA_{A,fast}$ inhibitory interneurons) which communicate via excitatory and inhibitory synapses. Worth noting is the presence of a new feedback loop with gain C_{ff}.

synaptic population. These connections agree with those proposed by Wendling et al. (2002) but with the addition of the new self-loop C_{ff}.

An important aspect of the model is the external inputs. Since inputs originate from pyramidal neurons in other cortical areas, in the following we will assume that they always act via excitatory synapses (hence, with impulse response $h_e(t)$). In previous works (Ursino et al., 2007; Zavaglia et al., 2008), we assumed that inputs target pyramidal cells. However, lateral connections in the cortex target all layers (Felleman and van Essen, 1991), hence inputs can actually reach both pyramidal cells and excitatory interneurons as well as inhibitory interneurons (David et al., 2005). For brevity, in the following, we will consider only inputs to pyramidal neurons and to fast inhibitory interneurons. A parameters sensitivity analysis has been performed also on inputs to slow inhibitory and excitatory interneurons, but is not reported since it did not produce appreciable changes in model dynamics. This aspect will be further analyzed in the Discussion section.

In conclusion, compared with the model described in our previous work (Zavaglia et al., 2008), the new "complete model" has two changes: (i) fast inhibitory interneurons may receive an external input (say $u_f(t)$) from pyramidal neurons of other populations and (ii) fast inhibitory interneurons exhibit a negative self-loop, i.e., they not only inhibit pyramidal neurons (as in Wendling model), but also inhibit themselves. The final model is displayed in Fig. 3. It corresponds to the following set of differential equations:

Pyramidal neurons

$$\frac{dy_p(t)}{dt} = x_p(t) \tag{2.12}$$

$$\frac{dx_p(t)}{dt} = G_e\omega_e z_p(t) - 2\omega_e x_p(t) - \omega_e^2 y_p(t) \tag{2.13}$$

$$z_p(t) = \frac{2e_0}{1+e^{-rv_p}} - e_0 \tag{2.14}$$

$$v_p(t) = C_{pe}y_e(t) - C_{ps}y_s(t) - C_{pf}y_f(t) \tag{2.15}$$

Excitatory interneurons

$$\frac{dy_e(t)}{dt} = x_e(t) \tag{2.16}$$

$$\frac{dx_e(t)}{dt} = G_e\omega_e\left(z_e(t) + \frac{u_p(t)}{C_{pe}}\right) - 2\omega_e x_e(t) - \omega_e^2 y_e(t) \tag{2.17}$$

$$z_e(t) = \frac{2e_0}{1+e^{-rv_e}} - e_0 \tag{2.18}$$

$$v_e(t) = C_{ep}y_p(t) \tag{2.19}$$

Slow inhibitory interneurons

$$\frac{dy_s(t)}{dt} = x_s(t) \tag{2.20}$$

$$\frac{dx_s(t)}{dt} = G_s\omega_s z_s(t) - 2\omega_s x_s(t) - \omega_s^2 y_s(t) \tag{2.21}$$

$$z_s(t) = \frac{2e_0}{1+e^{-rv_s}} - e_0 \tag{2.22}$$

$$v_s(t) = C_{sp}y_p(t) \tag{2.23}$$

Fast inhibitory interneurons

$$\frac{dy_f(t)}{dt} = x_f(t) \tag{2.24}$$

$$\frac{dx_f(t)}{dt} = G_f\omega_f z_f(t) - 2\omega_f x_f(t) - \omega_f^2 y_f(t) \tag{2.25}$$

$$\frac{dy_I(t)}{dt} = x_I(t) \tag{2.26}$$

$$\frac{dx_I(t)}{dt} = G_e\omega_e u_f(t) - 2\omega_e x_I(t) - \omega_e^2 y_I(t) \tag{2.27}$$

$$z_f(t) = \frac{2e_0}{1+e^{-rv_f}} - e_0 \tag{2.28}$$

$$v_f(t) = C_{fp}y_p(t) - C_{fs}y_s(t) - C_{ff}y_f(t) + y_I(t) \tag{2.29}$$

It is worth noting that we used a sigmoidal function centered at zero, which corresponds to the use of a variational model.

Model of connectivity among areas: the "coupled complete model"

In order to study long-range connectivity, let us consider two cortical areas (each described via Eqs. (2.12–2.29)), which are interconnected through long-range excitatory connections with a time delay. The presynaptic and postsynaptic regions will be denoted with the superscript k and h, respectively. The generalization to more than two regions is trivial. To simulate connectivity, we assumed that the average spike density of pyramidal neurons of the presynaptic area (z_p^k) affects the target region via a weight factor, W_j^{hk} (where $j=p$ or f, depending on whether the synapse target to pyramidal neurons or fast inhibitory interneurons) and a time delay of 10 ms, T. This is

achieved by modifying the input quantities u_p^h and/or u_f^h of the target region.

Hence, we can write

$$u_j^h(t) = n_j^h(t) + W_j^{hk} z_p^k(t - T) \quad j = p,f \tag{2.30}$$

$n_j(t)$ represents Gaussian white noise (in the present work: mean value $m_j = 0$ and variance $\sigma_j^2 = 5$) which account for all other external inputs not included in the model.

Results

Parameters sensitivity analysis on the population of $GABA_{A,fast}$ interneurons ("reduced model")

Fig. 4 shows the results of a parameters sensitivity analysis performed on C_{ff} and ω_f in Eq. (2.8). The analysis has been performed both with the linearized model described in the A single region model: a brief summary section (linearized solution) and the nonlinear model (Eq. (2.4), z, numerical solution). The left panels (a, c and e) show the square amplitude of the transfer function of the linearized model; the right panels (b, d and f) show a comparison between the linearized model (dashed line) and the output of the nonlinear model (continuous line); the latter has been computed, after numerical integration of the differential equations, as the PSD of the output divided by the PSD of the input u_f. The curves have been computed using three different values of parameters ω_f and C_{ff} (see Eq. 2.10).

As suggested by the theoretical study on the linearized model, the parameters sensitivity analysis confirms that the system has a resonance peak whose position can be changed within the frequency range of the γ-band (30–50 Hz) by acting on the two parameters. As a consequence, the input noise is amplified in correspondence of this peak and $GABA_{A,fast}$ interneurons exhibit an oscillatory activity in the γ band. Hence, $GABA_{A,fast}$ neurons can generate γ activity even if isolated from the other populations, thanks to the self-loop included in the model.

Parameters sensitivity analysis on a cortical area ("complete model")

Simulations performed in a previous paper (Zavaglia et al., 2006) demonstrate that the model of Wendling et al. (2002), stimulated with input white noise to pyramidal cells (u_p (t)), produces just a unimodal spectrum (i.e., a spectrum with a single well defined peak) whose position primarily depends on the synaptic kinetics (i.e., ω_e, ω_s, ω_f) parameters. Conversely, the model presented here (Fig. 3), including a self-loop between fast inhibitory interneurons, can generate more than one oscillatory rhythm within a single ROI.

An example is shown in Fig. 5a. Two rhythms are evident in the PSD, one in the β range and the other in the γ range. The parameters values used in the simulations are reported in Table 1 (Jansen and Rit, 1995). We used a value for the time constants of $GABA_{A,fast}$ interneurons of 13 ms, which is in accordance with in-vivo studies (White et al., 2000).

Generation of γ-band power

In order to identify the loops that are essential to obtain a rhythm in the γ band, we performed a parameters sensitivity analysis on the six gains which describe the strength of the connections among the four neural populations. In particular, the PSD was computed by assigning a value zero to each gain, while the other five gains are maintained at the basal value. The results show that, when connections from pyramidal cells toward excitatory interneurons (C_{ep}) or from $GABA_{A,slow}$ interneurons toward pyramidal cells (C_{ps}) are set to 0 (Figs. 5b and c), the two rhythms persist. When the connection from pyramidal cells toward $GABA_{A,fast}$ interneurons (C_{fp}) is set to 0,

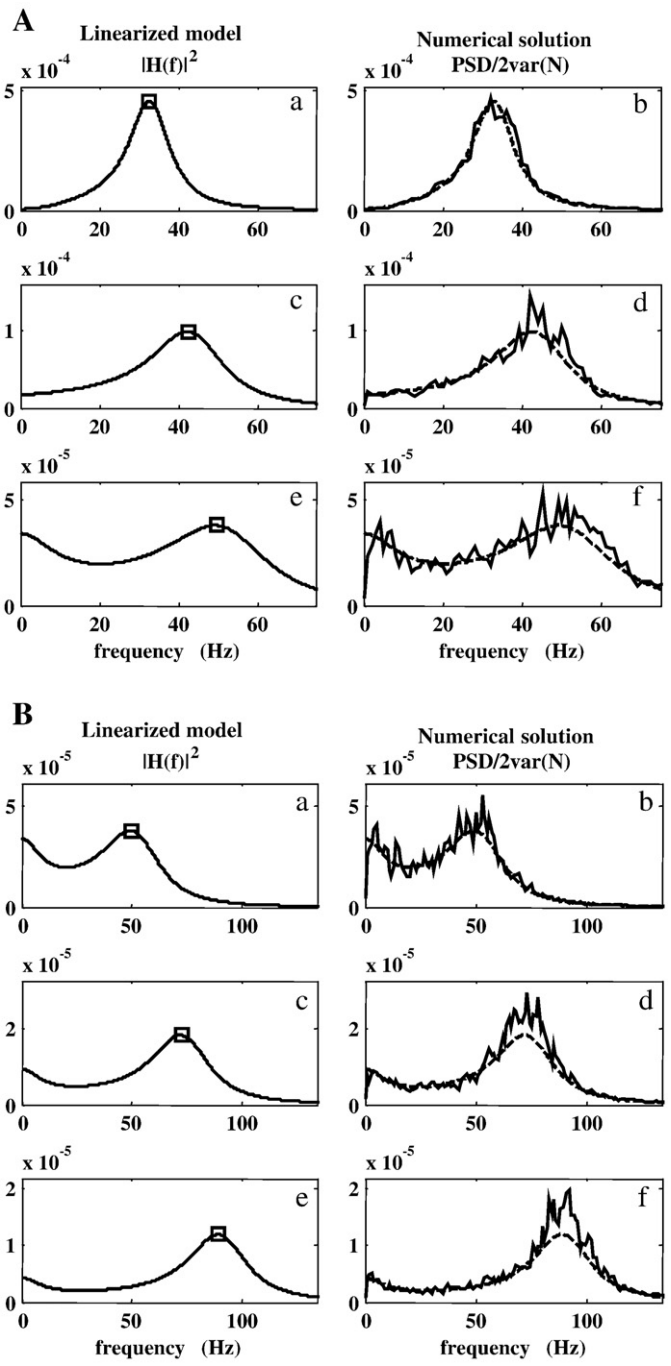

Fig. 4. Comparison between the analytical and numerical solutions obtained with the model of a single loop of $GABA_{A,fast}$ interneurons. For each row, different values of ω_f (respectively 40 s^{-1}, 70 s^{-1} and 100 s^{-1}, panel a) and C_{ff} (respectively 27, 54 and 81, panel b) have been used.

the two rhythms are not clearly distinguishable, but the power band is still fairly broad (0–40 Hz) (Fig. 5d). Conversely, when the connection from $GABA_{A,slow}$ interneurons toward $GABA_{A,fast}$ interneurons (C_{fs}) is cut (Fig. 5e), the two rhythms collapse in a single one oscillating in the γ band. Instead, when the connections from $GABA_{A,fast}$ interneurons to pyramidal cells (C_{pf}) or from $GABA_{A,fast}$ interneurons toward themselves (C_{ff}) are cut (Figs. 5f and g), the two rhythms collapse in a single one located at low frequencies, suggesting a crucial role for these connections in the generation of γ rhythm.

The previous simulations show that the presence of fast inhibitory interneurons with a self-loop is essential to generate a γ rhythm within a single region. However, these simulations were just

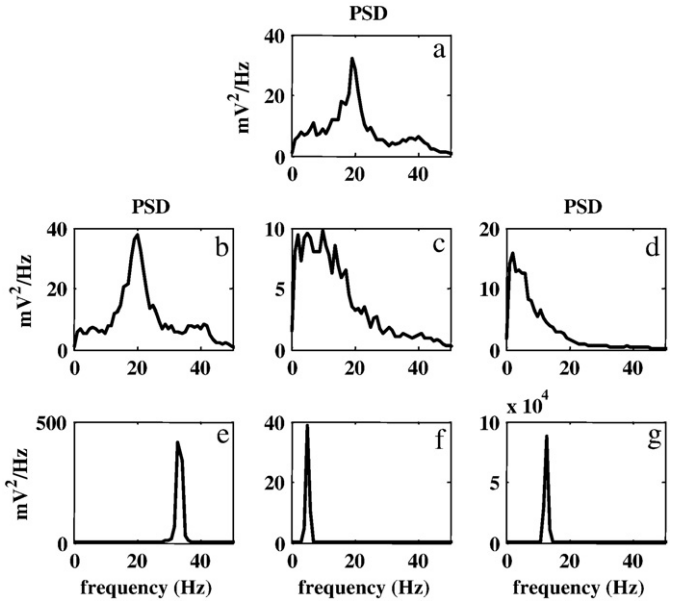

Fig. 5. PSD of a single region setting off some connections among neural populations. The first panel represents the output of the whole model with parameters as in Table l. The other six panels represent the power spectra respectively when $C_{ep}=0$, $C_{ps}=0$, $C_{fp}=0$, $C_{fs}=0$, $C_{pf}=0$, $C_{ff}=0$.

performed according to an ON/OFF criterion, i.e., by individually eliminating the contribution of single connectivity weights.

Hence, we performed a more exhaustive analysis on the whole connectivity parameter space. Here, simulations have been performed by systematically varying the seven parameters which represent the internal connectivity (except C_{ff}). For each parameter, we used six different values within a physiological range (0, 27, 54, 81, 108, 135), while the other parameters (ω_e, ω_s, ω_f, G_e, G_s, G_f) were maintained at the values reported in Table 1. Hence, the total number of points probed in the parameter space (D) was $6^7=279936$.

For each parameter set, three simulations have been performed: one for the Wendling model, another for the new model, and the last for a control model, that is, a model equal to Wendling model plus the white noise input for the $GABA_{A,fast}$ interneurons. The control model has been analyzed to verify that the differences between the model by Wendling and the new one are actually due to the $GABA_{A,fast}$ loop.

For each model and for each parameter set, we computed the PSDs.

The first analysis was devoted to ascertain the possibility to generate a significant power in the γ band by each model. To this end, for each parameter value, and for each model, we computed: (i) an *upper frequency* for the spectrum, defined as the frequency below which 95% of power is contained; (ii) an *average frequency* for the spectrum, defined as the frequency below which the spectrum contains 50% of its power. Results are presented in Fig. 6, in the form of a histogram showing the percentage of results for each frequency range. Results show that 95% of the power for Wendling's model and for the control model is always located between 0 and 25 Hz, whereas for a high percentage of simulations the new model shows significant power activation also in the γ band (Fig. 6a). Moreover for about 1/4 of the simulations, the new model generates half of the power at frequencies higher than 25 Hz (panel b). This means that the new model not only can generate γ activity, but it is also suitable for the generation of power spectral peaks in the γ band.

These results clearly demonstrate that only if $C_{ff}\neq 0$, we can produce an evident γ rhythm using physiological values for time constants, further supporting the importance of the new loop.

A further set of simulations has been performed by systematically varying parameter C_{ff} (i.e., strength of the inhibitory interneurons fast loop) from 0 to 236.25, while all other parameters are set at the same value as in Table 1. Results, not shown for briefness, demonstrate that the frequency of the second peak in the spectrum progressively increases from 30–40 Hz to 100–120 Hz by increasing C_{ff}, although at high values of this parameter the amplitude of the γ peak significantly decreases.

Bimodal spectra

A subsequent analysis was devoted to ascertain the possibility of generating two distinct peaks in PSD. This point has been handled by studying the transfer function of the linearized system (LS) around its

Table 1
Model basal parameters.

Parameter	Symbol	Value
Average gains (mV)	G_e	5.17
	G_s	4.45
	G_f	57.1
Time constants reciprocals (s^{-1})	ω_e	75
	ω_s	30
	ω_f	75
Numbers of synaptic contacts	C_{ep}	54
	C_{pe}	54
	C_{sp}	54
	C_{ps}	67.5
	C_{fp}	54
	C_{fs}	27
	C_{pf}	540
	C_{ff}	27
Sigmoid saturation (s^{-1})	e_0	2.5
Sigmoid steepness (mV^{-1})	r	0.56
Time delay (ms)	T	10

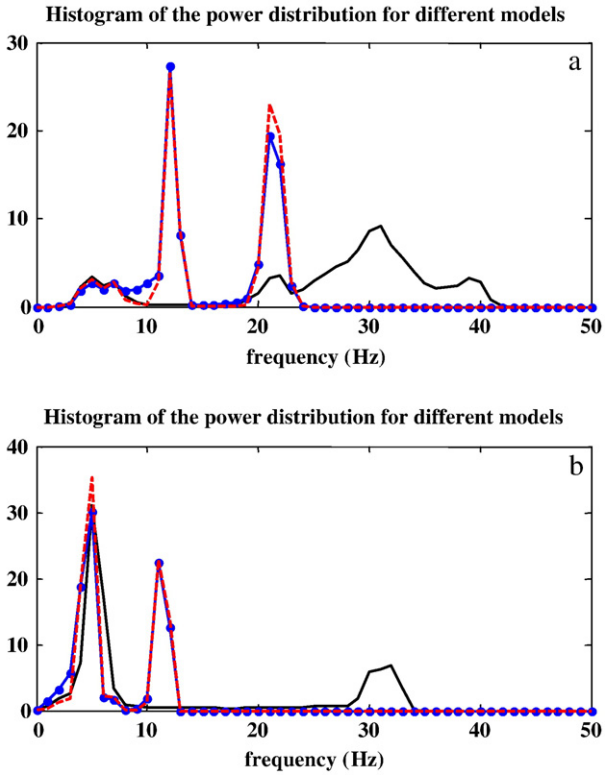

Fig. 6. Panel a shows a histogram of the power distribution obtained with the model by Wendling (dashed line), with the new model (continuous line) and with the control model (marked line). For each frequency f, the figure indicates the percentage of simulations in the parameters space D for which 95% of the power is below f. Similarly, panel b indicates the percentage of simulations in the parameters space D for which 50% of the power is below f. See text for details (Parameters sensitivity analysis on a cortical area ("complete model")).

equilibrium points. For each set of parameters, the equilibrium points have been calculated and the stability evaluated (Hartman-Grobman theorem) looking at the real part of eigenvalues. About 25% of the parameter sets gives at least one stable LS for the model by Wendling, while this percentage rises to about 54% for the new model. Among the stable LSs, we looked for those that could generate at least two distinct resonance peaks. To this end, the 8th degree polynomial at the denominator of the transfer function has been factorized in four 2nd degree polynomials $DEN_i(s) = (s - p_{i,1})(s - p_{i,2})$. Every $DEN_i(s)$ block can generate a resonance if it has two complex conjugate poles that verify the following constraints: $Re(p_i) < 0$, $Re(p_i) > -|Im(p_i)|$ (damping factor less than $1/\sqrt{2}$). Results show that these constraints are verified in about 12% of the simulations in the new model, but just in 0.04% (118 sets of parameters) in the model by Wendling. Hence, the new model is much more suitable to produce two distinct resonance peaks than the former one. Finally, we further looked for those resonance peaks which are at least 10 Hz apart from one another, and which exhibit a damping factor $\delta < 0.1$: these last stricter constraints ensure the presence of two well evident peaks in the spectra. An example for the new model when the latter constraints are satisfied is shown in Fig. 7. However, these conditions are limited (less than 1% of the simulations) even in the new model. Most conditions characterized by two well defined peaks in the spectra are associated with unstable equilibrium points, i.e., the development of limit cycle dynamics. The latter analysis may be the subject of future work.

Role of time constants

A last set of simulations has been performed to show the role of the time constant of fast synaptic kinetics. To this end, PSD has been computed in the three models using the values of connectivity strength reported in Table 1, and progressively reducing the time constant τ_f from 13 to 1 ms. Results, shown in Fig. 8, confirm that the present model can produce a significant power in the γ band for all values of τ_f. If τ_f is reduced down to 1 ms, a broadband spectrum can be observed. Conversely, Wendling model and the control model can produce significant power in the γ band only if the time constant used for fast synaptic kinetics is as low as 1–2 ms.

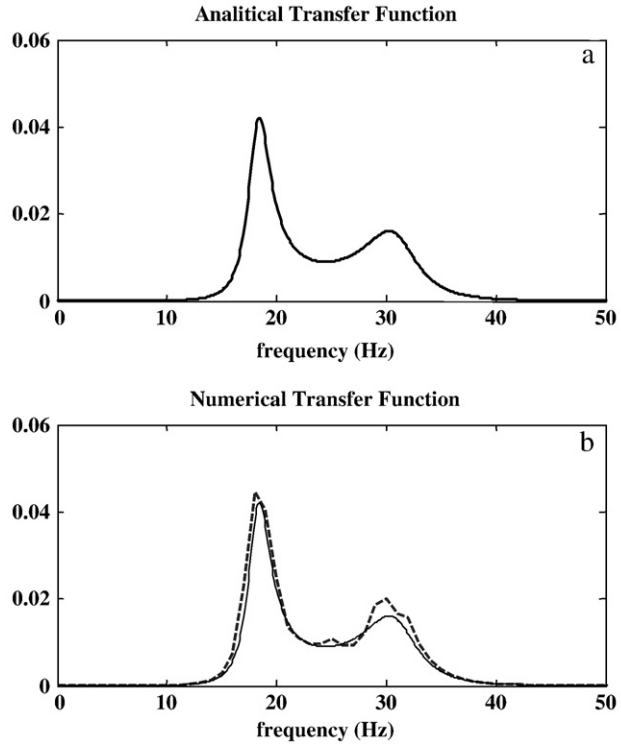

Fig. 7. Example of a bimodal spectrum generated with the new model. Panel a shows the squared modulus of the transfer function (continuous line) of the associated linearized system around a stable equilibrium point. Panel b shows the squared modulus of the transfer function computed as the PSD of the numerical solution of the model divided by the PSD of the input noise (dashed line). In panel b the continuous line represents the same plot as in panel a.

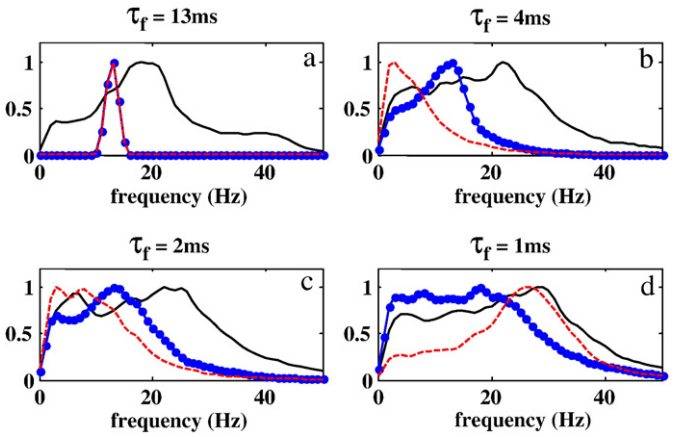

Fig. 8. Power spectra of the model by Wendling (dashed line), of the new model (continuous line) and of the control model (marked line), when the time constant of $GABA_{A,fast}$ interneurons is changing. The values of the other parameters are from Table 1.

Connectivity between two cortical areas ("coupled complete model")

Further simulations were performed to study the transmission of rhythms from one region to another as a consequence of connectivity with time delay between the two regions. In these simulations, parameters were given so that populations exhibit limit-cycle behavior (i.e., oscillations arise as the consequence of internal instability), to emphasize rhythm generation and transmission (see also the analysis in section 3.2).

Fig. 9 shows the behavior of a model composed of two interconnected regions. In each panel, the first two columns represent the PSD of the two regions; the third is the coherence function while the fourth column represents the connectivity diagram. In all simulations, parameter C_{pf} is set to 540 in the first region, whereas it is set to 108 in the second one. All other parameters have the same values as in Table 1. As a consequence of these choices, the first region exhibits two rhythms (the first in the β and the second in the high γ range) while the second region exhibits only one narrow rhythm in the low γ range. The results of different simulations are shown, with the connectivity strength from the second to the first region progressively increased. Moreover, the connectivity was directed either to fast inhibitory interneurons, to pyramidal neurons, or to both. The most interesting result is that if the connectivity is sent toward pyramidal cells the rhythm is not induced in the target region and also the coherence function is low (panels d–f and m–o), whereas if the connectivity is sent to $GABA_{A,fast}$ interneurons, the presence of a new induced peak is evident (panels g–l) and the first region exhibits three simultaneous rhythms.

Fig. 10 shows another example of connection between two regions. In these simulations, the parameter C_{pf} of the second region has been set to 0 in order to obtain a rhythm around 5 Hz. This region could simulate an area which oscillates at low frequency, for example the thalamus. It is worth noting that, if the connections are sent to $GABA_{A,fast}$ interneurons, the first region exhibits three rhythms, with one in the θ band (5 Hz) induced by the second region. This behavior is reflected in the coherence function.

Fig. 11 shows the effect of connectivity among three regions. All the regions are simulated with the parameters reported in Table 1, but the first region has $C_{pf} = 0$ to reproduce the activity of an area with a rhythm in the θ band and the third region has $C_{pf} = 108$ to reproduce

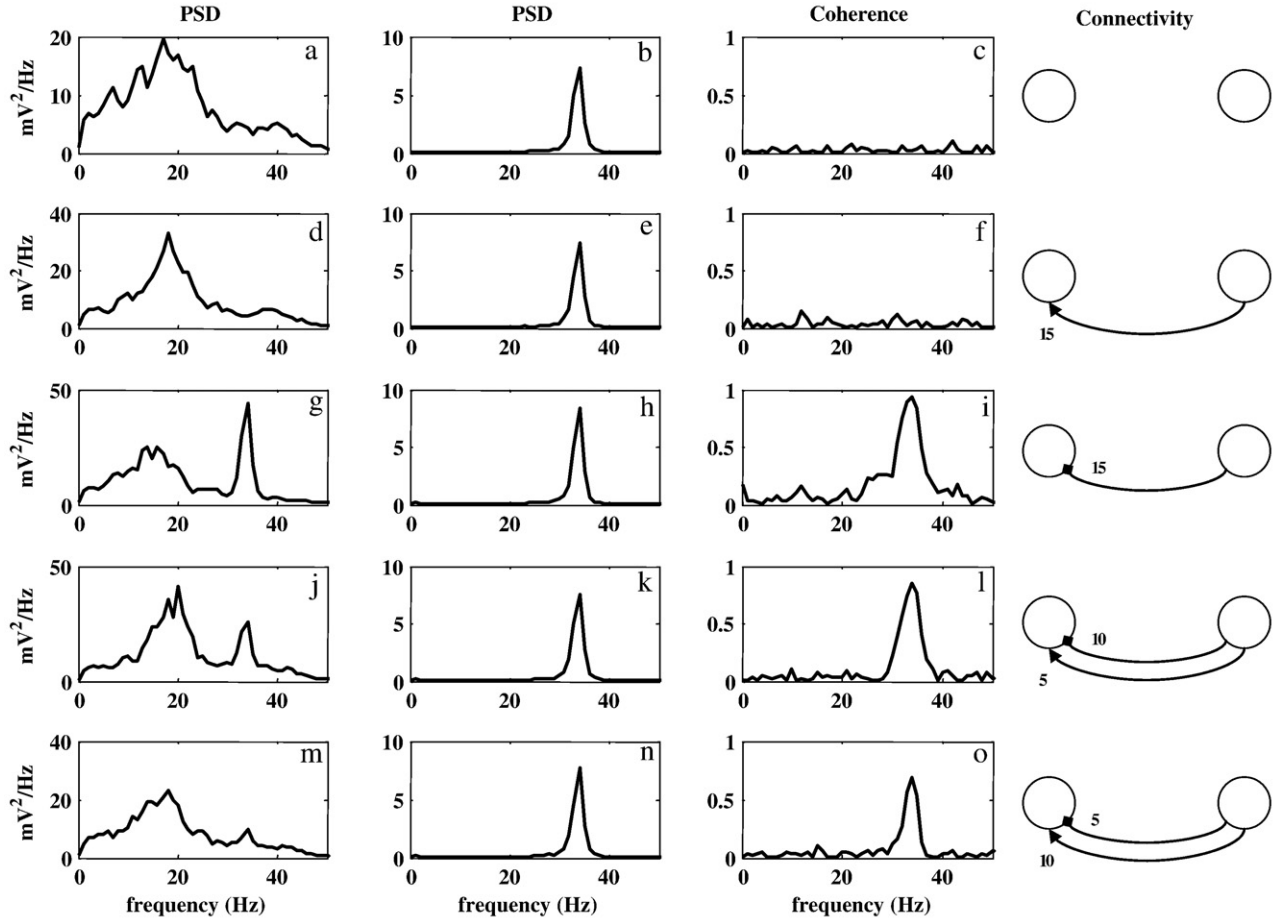

Fig. 9. PSD of two regions (first region in the first column (panels a, d, g, j, m) and second region in the second column (panels b, e, h, k, n)) communicating by different connectivity patterns. The coherence between the two regions is represented in the third column (panels c, f, i, l, o); the connectivity patterns are represented in the fourth column. The arrow indicates connectivity toward pyramidal cells, the square indicates connectivity toward $GABA_{A,fast}$ interneurons. See the text for other parameters values.

the activity of an area which oscillates in the γ range. It is worth noting that in this case the PSD of the second region exhibits a multiple spectrum (with intrinsic and induced rhythms), comprehensive of the contributions from all the regions. The coherence is high in correspondence of the induced rhythms.

Of course, real connections in the cortex often exhibit feedback loops. A comprehensive study of all the possible combinations of connectivity patterns among two, three or even more regions, would require a combinatorial explosion of possibilities. For the sake of brevity, we just investigated an example of two regions with feedback connections to show that this kind of connectivity does not change the results dramatically in comparison to unidirectional connectivity, while an extensive study could be addressed in future works.

In Fig. 12, the upper panels (panels a–l) analyze the case in which one region oscillates in the θ band and the other in the γ band. The bottom panels (panels m–r) analyze a case in which one region oscillates in the low γ band and the other in the high γ band. In both cases, multimodal spectra can be produced in both regions if connections have a sufficient strength. In this case too, connections to fast inhibitory interneurons are more efficient to cause rhythm propagation. It is worth noting that feedback connections may also induce a shift in one peak (by way of example, let us see the third row, where a peak in the β band appears, which was not originally present in either of the two regions).

Finally, Fig. 13 shows a comparison between a real PSD obtained on a healthy volunteer during a simple movement task (taken from Zavaglia et al., 2008) and a spectrum simulated with a model of two interconnected regions. In this case, we did not try a best fitting, but we simply looked for a manual adjustment of connectivity parameters to show the similarity between real spectra and simulated ones. This result emphasizes that spectra similar to those found in vivo can be obtained with a parsimonious model, and just adjusting a few connectivity weights.

Discussion

The present work extends the possibilities offered by neural mass models to simulate real power density spectra, and to investigate effective connectivity patterns. The main new issues are concerned with: (i) the possibility to generate γ-rhythms using just a chain of fast-inhibitory interneurons, without the presence of the other neural populations; of course, in real physiological conditions the frequency of this rhythm is not fixed, but is modulated by the other populations; (ii) the possibility to engender multiple rhythms in the same model, without the need to include multiple synaptic kinetics; and (iii) the role played by inputs converging into fast inhibitory interneurons to propagate rhythms from one region to another.

In the following, each of these items is discussed separately:

(i) *γ-rhythm generation*: Our theoretical analysis stresses the possibility to generate a peak in PSD within the γ-band in a simple way, by just introducing an inhibitory loop among fast interneurons. This loop is physiologically motivated by the presence of significant interconnections between fast basket cells, as observed in the hippocampus (Cobb et al., 1997) and in the neo-cortex (Kisvarday et al., 1993). The idea that a self-loop of one population to itself (frequently used in competitive neural networks) can enrich the

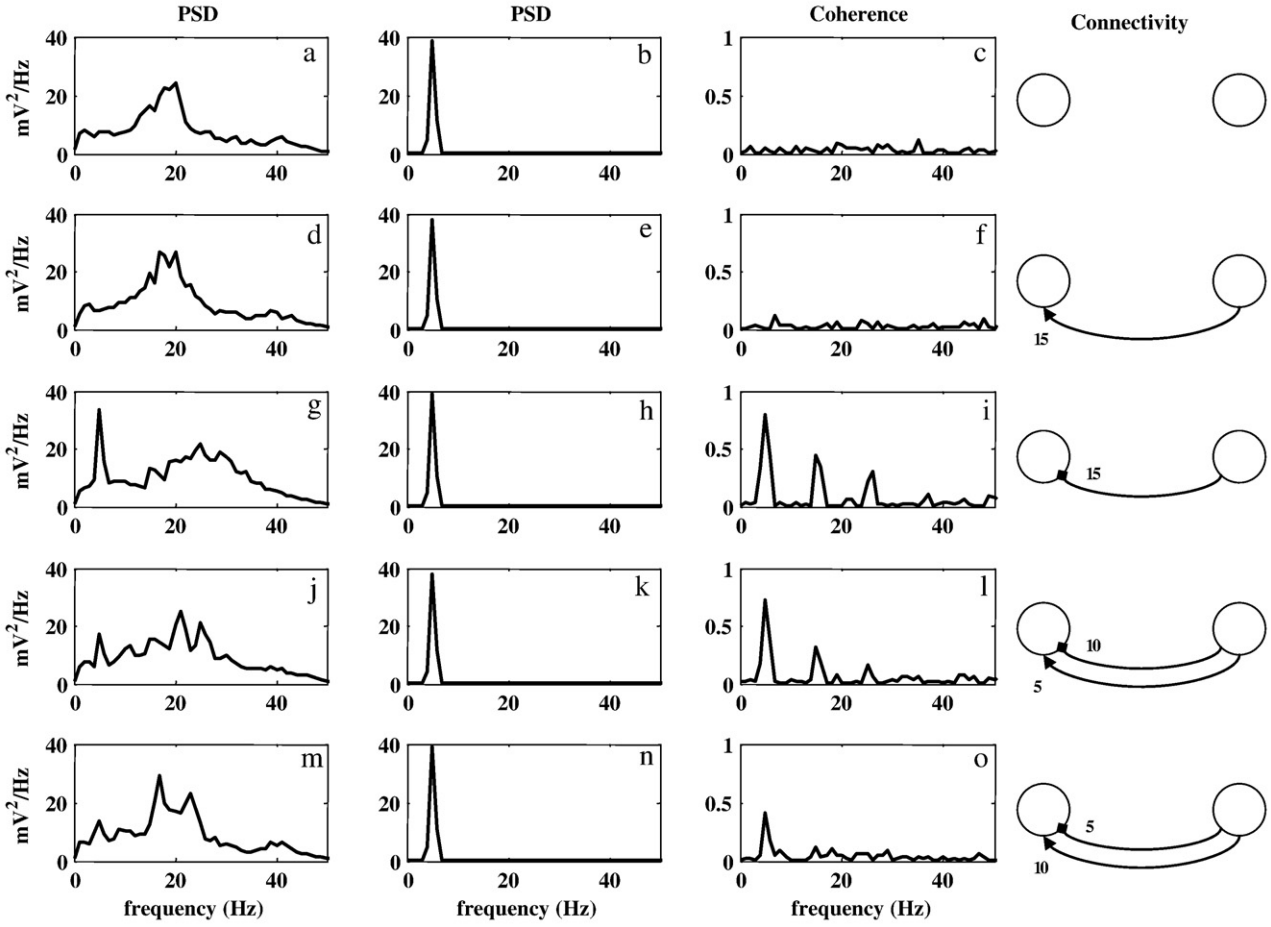

Fig. 10. PSD of two regions communicating by different connectivity patterns. In this simulation, the values of the parameters are the same as in Fig. 9 except for the parameter C_{pf} of the second region, which has been changed ($C_{pf}=0$) in order to obtain a rhythm around 5 Hz. All the panels represent the same quantities as in Fig. 9.

dynamics of neural mass models was already exploited by Sotero et al. (2007) in their recent model of overall brain dynamics. However, these authors included a loop between pyramidal cells only, assuming that, at a large scale, "pyramidal-to-pyramidal connections become increasingly important, accounting for the majority of intracortical fibers." A similar loop among inhibitory interneurons has been used by Moran et al. (2007) to simulate γ rhythms; however, these authors did not use two distinct populations of interneurons; in particular, they did not simulate interneurons with $GABA_{A,fast}$ kinetics. A large amount of modeling and experimental work suggests that fast inhibitory networks play a significant role in the genesis of γ rhythms (Bartos et al., 2007; Jefferys et al., 1996; White et al., 1998; Whittington et al., 1995).

Our analysis underscores that γ oscillations can be obtained using physiological values for the time constant of fast inhibitory synapses (range 10–20 ms), contrarily to previous works (Wendling et al., 2002; Zavaglia et al., 2006, 2008) where one needed to use very small values (a few ms) for the time constant of $GABA_{A,fast}$ interneurons. Furthermore, the lower the time constant, the higher the oscillation frequency. This result agrees with data reported by Whittington et al. (1995) (see also Fig. 4 in Jefferys et al., 1996). These authors, both via computer simulations in integrate and fire neural networks and in experimental trials during pentobarbital infusion, observed that the frequency of γ rhythms is inversely related with the time constant of the inhibitory post-synaptic current. Moreover, the value of the time constants in their work is close to that used in our model.

A further interesting result of our analysis is that the frequency of γ-rhythms is directly related with the connectivity strength among fast interneurons (i.e., parameter C_{ff} in Fig. 2). If this parameter is increased by twofold or threefold with respect to its basal value, the model predicts oscillations in the ultra γ range (about 70 Hz). For even greater values of parameter C_{ff}, oscillation frequency may increase up to 80–100 Hz, although the amplitude of the PSD peak significantly decreases. This dependence of frequency on connectivity requires further experimental validation.

It is worth noting that Rennie et al. (2000), using a continuum model of electrical activity in the cortex, also ascribed the emergence of γ rhythm to a resonance near 40 Hz. However, in their model the resonance depends on a modulation of synaptic strength, hence to a different mechanism compared with that exploited in the present work.

In conclusion, the model ascribes the occurrence of a γ rhythm to the presence of a resonance occurring within the network of fast inhibitory interneurons, here described by means of a simple feedback loop. In the linearized model, the frequency and amplitude of the resonance peak depend on the time constant of the $GABA_{A,fast}$ synapses and on the strength on reentrant connections between these interneurons. In the non-linear model, these quantities can also be modulated by the excitatory input to the fast interneurons: the latter may affect the working point in the sigmoidal characteristic, thus altering the loop gain.

Of course, the mechanism exploited in the present model to generate γ rhythms may not be the unique one; alternative mechanisms may be effective to generate γ rhythms in different conditions, as reviewed by Jefferys et al. (1996). These may include a recurrent inhibition between an excitatory and an inhibitory

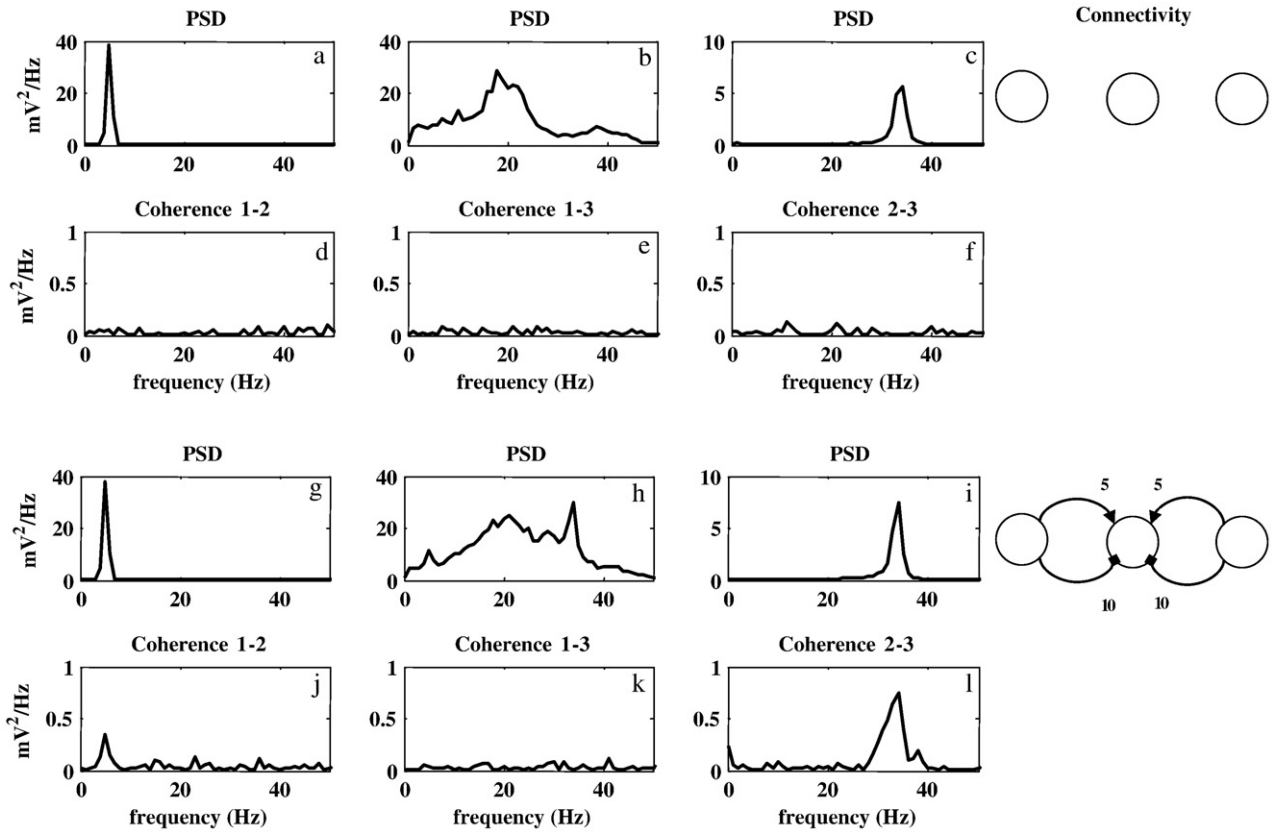

Fig. 11. PSD of three regions communicating by different connectivity patterns. The first region (panels a, d, g, l) is simulated with a value of $C_{pf}=0$, the second region (panels b, e, h, k) with a value of $C_{pf}=540$ and the third region (panels c, f, i, l) with a value of $C_{pf}=108$. The other panels represent the connectivity patterns and the coherences between the regions.

population, or the presence of intrinsic pacemaker cells. The first mechanism is widely exploited in classic models of neural oscillators (such as the Wilson-Cowan oscillator (Wilson and Cowan, 1972)) and is commonly adopted in more traditional neural mass models (Freeman, 1978; Lopes da Silva et al., 1974). However, to produce γ rhythms, this mechanism must assume the presence of very small time constants for the synapses. Particularly, results in Fig. 8 show that γ rhythms in power spectral density can be generated using the Wendling model (Wendling et al., 2002), but one needs a time constant for fast inhibitory interneurons as low as 1–2 ms. For what concerns the second mechanism, examples of intrinsic pacemaker cells in the cortex are well documented (Gutfreund et al., 1995; Llinas et al., 1991), although we are not aware of their use within neural mass models.

Finally, it is remarkable that not only fast interneurons, but also gap junctions can be important for some forms of γ oscillations (Wang and Buzsaki, 1996). Probably gap junctions increase the oscillation power, although are not necessary for their generation (Bartos et al., 2007). Their effect may be that of increasing coupling between interneurons populations, i.e., an increase in the coupling terms C_{ij} of our model.

(ii) *Multiple rhythms in the same ROI*: If the four populations (pyramidal neurons, excitatory interneurons, slow and fast interneurons) which constitute a cortical column are connected with realistic connectivity loops (Fig. 3) the model can produce two simultaneous rhythms: the first, in the γ band, can be ascribed to a resonance of fast inhibitory interneurons; a second, at lower frequencies (in the α band or β band), emerges from the other feedback loops (i.e., loops engaging pyramidal neurons, excitatory interneurons and slow inhibitory interneurons). It is worth noting that this "intrinsic rhythm" is that obtainable from the traditional Jansen and Rit model (Jansen and Rit, 1995) and represents the core of most recent studies using neural mass models (Babajani and Soltanian-Zadeh, 2006; David et al., 2005; David and Friston, 2003; Sotero et al., 2007; Zavaglia et al., 2006).

Jefferys et al. (1996), in their review paper on mechanisms generating γ rhythms, suggested that "the fact that inhibitory networks can sustain a rhythm in the γ frequency range… separates the synchronizing control or clock from the specific neural processing of information." This idea substantially agrees with the results emerging from our model: a higher frequency rhythm originating in the fast-inhibitory loop modulates (and is modulated by) a slower rhythm within the same region, originating from slower synapse time constant.

The parameter sensitivity analysis shown in Figs. 5 and 6 supports this viewpoint. If parameter C_{ff} is set at zero, the model cannot generate a significant power in the γ-band (using physiological values of time constants) but all power is concentrated below 25 Hz. Conversely, a significant power above 30 Hz can be obtained with many combinations of parameters if C_{ff} is significantly different from zero. In the latter condition, if connectivity between pyramidal, excitatory and slow-inhibitory interneurons is changed, one can observe evident changes in PSD within the α and β bands, whereas the PSD still exhibits a significant contribution in the γ band (panels b and c in Fig. 5).

Analysis of the poles in the linearized model also supports a pivotal role for parameter C_{ff}. Only the present model (with $C_{ff}\neq 0$) can frequently produce two resonant peaks if linearized around a stable equilibrium point (Fig. 7) whereas with $C_{ff}=0$ the presence of distinct resonant peaks in the transfer function becomes very rare. Nevertheless, our analysis also suggests that, in most conditions, the present model (as well as the Wendling model) does not exhibit stable equilibrium points, but its behavior arises from limit-cycle oscillations. We did not explore these aspects in the present

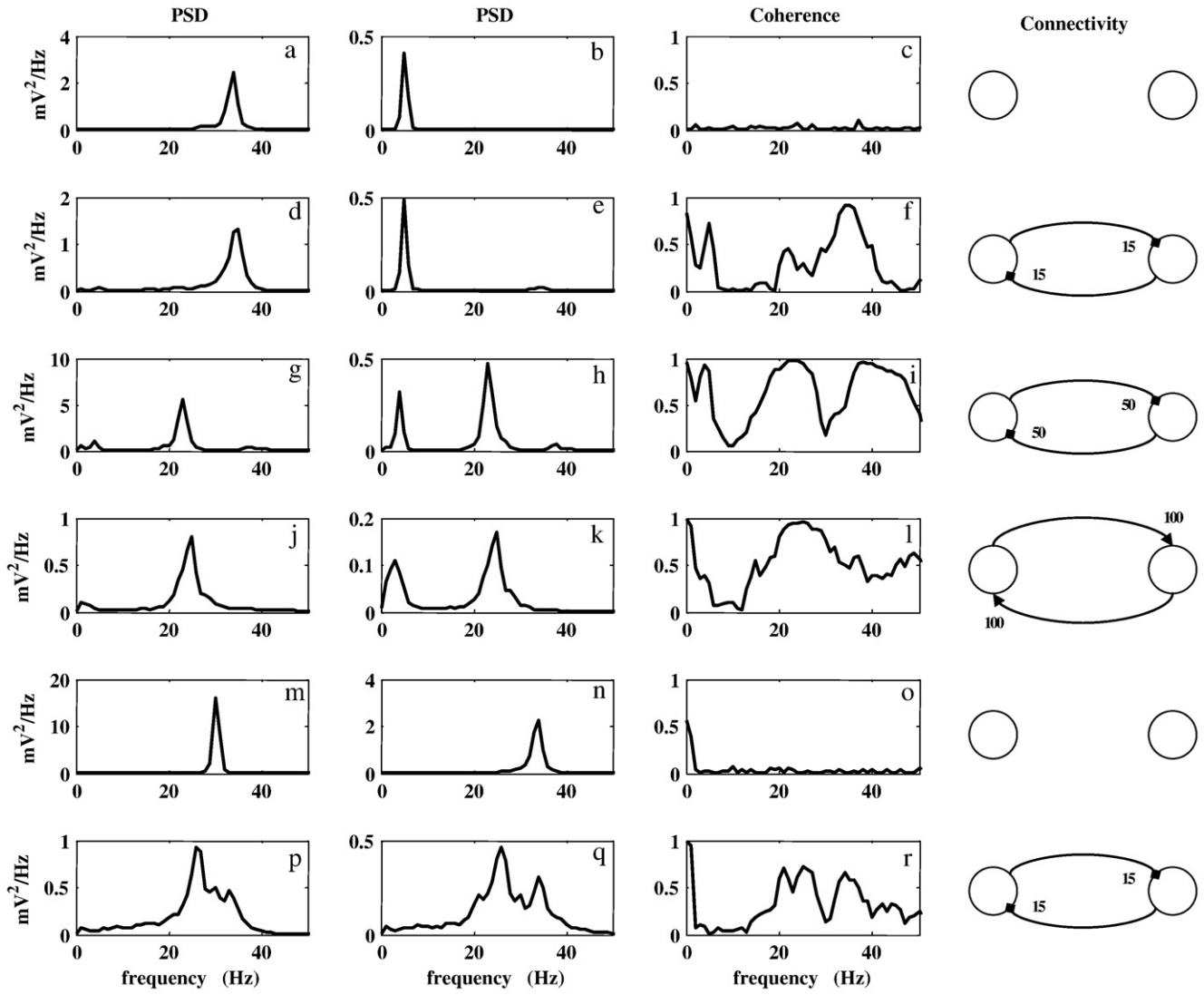

Fig. 12. PSD of two regions communicating by different connectivity patterns. In the first 4 rows (panels a–l), the first region is simulated with a value of $C_{pf}=108$ while the second region with a value of $C_{pf}=27$. In the last two rows (panels m–r), the first region is simulated with a value of $\omega_f=55\ s^{-1}$ and with a value of $C_{pf}=108$ while the second region with a value of $\omega_f=75\ s^{-1}$ and a value of $C_{pf}=108$. All the panels represent the same quantities as in Fig. 9.

work, but they might be the subject of future more refined theoretical analyses.

Definitely, the previous analysis suggests that the model can generate a variety of PSDs, with two simultaneous rhythms ($\alpha+\gamma$, or $\beta+\gamma$) or even a wide-band spectrum, by simply altering internal connectivity parameters, without the need of any ad hoc changes in the synaptic time constants. These bimodal oscillations may arise from the presence of two resonant peaks in the linearized model or from a more complex non-linear limit cycle dynamics.

(iii) *The role of fast interneurons on rhythm transmission between ROIs*: A remarkable result of our simulations is the pivotal role played by long-range excitatory connections which terminate into fast inhibitory interneurons. Indeed, the present work introduces a new testable hypothesis that we cannot find in previous studies: i.e., that excitatory input to fast inhibitory interneurons plays a fundamental role to transmit rhythms from one region to another. Our results clearly show that a moderate synapse from pyramidal neurons in the pre-synaptic ROI to fast inhibitory interneurons in the post-synaptic ROI is able to transmit rhythms very efficaciously, as observable in the spectrum of the target region and in the coherence between EEGs in the two regions. Conversely, excitatory synapses from pyramidal to pyramidal neurons are less effective in rhythms transmission, as revealed by the low value of coherence between the two ROIs. Only if the strength of synapses is increased by one order of magnitude, pyramidal to pyramidal connections become really efficacious and one can observe a high coherence (above 0.5) in the frequency band interested by the rhythm.

According to the literature (Felleman and van Essen, 1991), long-range connectivity originates exclusively from pyramidal neurons, but may target to different populations of neurons depending on the type of connection. In the present study, we focused attention just on two of these connections (from pyramidal to pyramidal and from pyramidal to fast inhibitory) to study two target populations with different time constants. Time constants, in fact, are the main determinants of population dynamics. However, we repeated the simulations in Figs. 9–12 assuming that connectivity reaches also the slow inhibitory and the excitatory interneurons (these are not presented for briefness). The presence of these further inputs does not appreciably modify the previous results.

We claim that the reason why a population of fast interneurons may be so efficacious to receive an external rhythm, and transmit it to other populations in the same area (especially to pyramidal cells), can be found in its fast dynamics, which allow the preservation of the overall spectral content of the external rhythms. Moreover, the

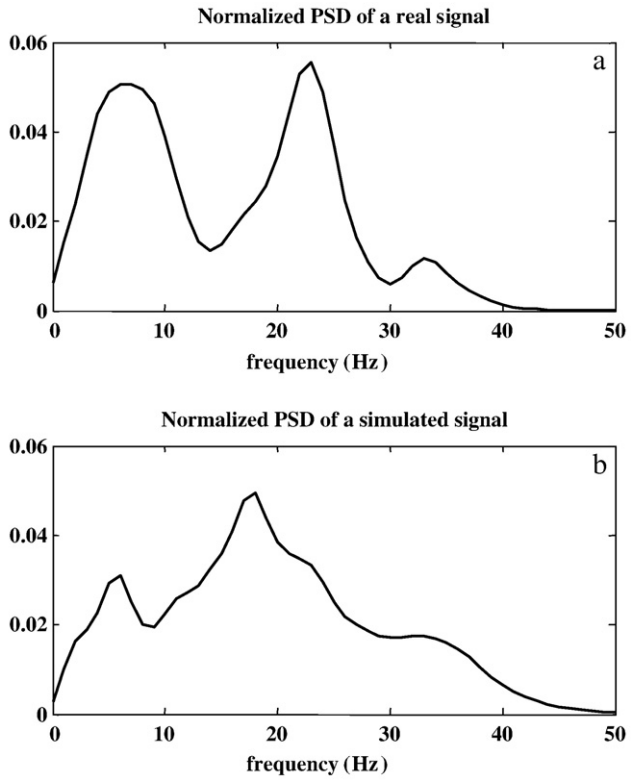

Fig. 13. Panel a shows the power spectrum of a real cortical signal. Panel b shows the spectrum of a signal simulated with a model of two interconnected regions: the first region has an intrinsic α rhythm, while the second one oscillates in β and γ ranges. The parameters which have different values from those reported in Table 1 are: for the first region $\omega_e = 120\ s^{-1}$, $\omega_f = 55\ s^{-1}$, $C_{fp} = 121.5$, $C_{fs} = 40.5$, $C_{pf} = 27$, $C_{ff} = 135$; for the second region $\omega_f = 55\ s^{-1}$. The weight factors are: $W_p^{21} = 200$, $W_p^{12} = 90$, $W_f^{21} = 0$, $W_f^{12} = 0$. When the two regions are connected to each other, the second one shows a power spectrum similar to the real one.

inhibitory loop of $GABA_{A,fast}$ interneurons with themselves is faster compared to the loop composed of $GABA_{A,fast}$ interneurons and pyramidal cells; for this reason, the perturbations that reach fast inhibitory interneurons have a stronger effect on the entire dynamics of the system.

It is worth noting that the term "efficient connection" has been used here just to denote the capacity to propagate a rhythm from one population to another. Of course, it is does not necessarily implies efficiency in a wider computational meaning, i.e., the capacity to maximize information transmission with a reduced wiring cost (such as evaluated in "small world network"; see Achard and Bullmore, 2007).

The observation that rhythm transmission is particularly efficient when connections target fast inhibitory interneurons may have a cognitive significance. In fact, according to the classic distinction developed by Felleman and van Essen (1991), connectivity may vary depending on the hierarchical level along the processing stream. In particular, in the visual cortex lateral connections target all layers, while top-down (backward) connections target supra-granular and infra-granular layers. In both cases, inhibitory interneurons can be among the target cells. Conversely, bottom-up (forward) connections terminate in layer 4, making synapses only to excitatory interneurons. Hence, according to Felleman and van Essen schema, model predicts a stronger capacity to transmit rhythm via lateral and top-down connections, but poorer capacity via forward connections. This distinction may have a cognitive role, suggesting that rhythm transmission (especially in the beta and gamma ranges) may be especially important in high level cognitive processes, which involve lateral connections among regions at the same hierarchical levels, and top-down influences from higher hierarchical centers.

An important aspect, which deserves attention, is whether multi-modal spectra, as those obtained in the present study, are actually found during real measurements in vivo. Indeed, several recent studies show real spectra in cortical regions similar to those reported in Figs. 9–12. Spectra with two distinct peaks are presented in Rowe et al. (2004) (see Fig. 4 in that work). In previous papers of our group, we tried to fit real spectra obtained after localization of the cortical sources, starting from high-density scalp EEG during simple movement tasks (Ursino et al., 2007; Zavaglia et al., 2008). Frequently, these spectra exhibited multiple peaks, in the α, β and γ bands (the reader can look at Fig. 4 in Zavaglia et al. (2008), for various examples). An exemplum of a real spectrum (taken from Zavaglia et al., 2008) is shown in Fig. 13 and compared with a PSD obtained with a model of two interconnected regions. In this figure, we did not try an automatic best fitting, but we simply adjusted connectivity parameters manually to arrive at an acceptable qualitative agreement. Best fitting of the present model to real spectra will be the subject of future model applications, maybe through the use of Bayesian estimation techniques (Moran et al., 2008).

A recent work by Rosanova et al. (2009), using TMS stimulation in human volunteers, further supports the existence of different rhythms (α, β and γ) in different cortical regions, and the possibility that rhythms are propagated from one region to another via effective connectivity pathways. In particular, TMS evoked an α-band oscillation in the occipital cortex, a β-band oscillation in the parietal cortex and a β/γ-band oscillation in the frontal cortex, but each region could also receive a different rhythm (thus showing multimodal spectra) from other regions via brain connections.

In the present work, we studied both uni-directional (Figs. 10 and 11) and bi-directional (Fig. 12) connections. In the first case, the target population may receive a further rhythm (besides its intrinsic rhythm) from the other population, with the appearance of a more complex spectrum. This should be easily observable in vivo (see Rosanova et al., 2009). The case of bi-directional connection is more complex, since the spectra of both populations are simultaneously affected (let us consider, for instance, the exemplum in the bottom panel in Fig. 12). In this condition, it may be difficult to assess the mechanisms leading to multimodal spectra from in vivo data, without the use of mathematical models and algorithms for effective connectivity estimation. This paper wishes to represent a new step in that direction.

Finally, at the end of this discussion we wish to point out some limitations of our work and lines for future improvements.

The present model is basically derived from the model by Wendling et al. (2002), and differs from the recent model by Moran et al. (2007, 2009, 2008) due to the presence of inhibitory interneurons with $GABA_{A,fast}$ synaptic kinetics. We are aware that the model by Wendling et al. was originally proposed with reference to the hippocampus, and that some differences may exist between the hippocampus and the cortex. Nevertheless, there are several reasons which justify the use of the Wendling model for the cortex too, and the extension and improvement we propose in the present paper.

First, fast inhibitory interneurons not only represent a significant portion of GABAergic interneurons in the hippocampus (Freund and Buzsaki, 1996) but they are also present in the cerebral cortex (see Gonzalez-Burgos et al., 2005; Thomson et al., 1996). Second, several experimental studies used receptor antagonists to analyze individual mechanisms involved in neural oscillations; their results suggest that similar cellular and network mechanisms, as those seen in the hippocampus, generate γ oscillations in the cortex too (Bartos et al., 2007; Cunningham et al., 2003; Whittington et al., 1995). The previous two points support the idea that fast $GABA_A$ mechanisms operate in the cortex (as in Wendling model of the hippocampus) and

that they have a role in generating γ rhythms both in the hippocampus and in the cortex via similar mechanisms.

Of course, other types of neurons exist in the cortex and in the hippocampus, besides the four populations included in the Wendling model. At the present stage of our knowledge, a four population model may represent a good compromise between simplicity and completeness, since it encompasses all main dynamical aspects (i.e., the main types of time constants). However, inclusion of a larger number of neuron populations, each with its own synaptic dynamics, might improve the physiological reliability of neural mass models in future years and might represent a subject of interesting future activity.

Finally, it is remarkable that other authors in the past decades developed significant models to describe EEG spectra based on a "neural field approximation." The basic idea of these models is that the number of neurons in the cortex is large and the density of synaptic connections is high. Hence, these models consider the cortex as a continuum and use a set of nonlinear partial differential equations in space and time to describe the spatiotemporal evolution of neural activity. These models, with inclusion of fast inhibitory kinetics to simulate γ-band oscillations, might allow a further more complete analysis of brain rhythms, illustrating conditions in which rhythms may propagate, amalgamate or dissipate in a continuum space. This aspect may also represent an important subject of future work.

In conclusion, the present study proposes a new and simple method to generate γ rhythms within neural mass models, without the need to modify synaptic kinetics. In particular, three different conditions have been analyzed with the model. In the first (named "reduced model") we just considered connectivity among fast interneurons taken alone, and demonstrated that this model can produce a gamma rhythm per se. In a second condition (named the "complete model") we simulated the behavior of a single ROI (mimicked through the interaction among four populations) and showed that this model can produce a spectrum with two distinct peaks (in the beta and gamma ranges, or in the alpha and gamma ranges). In particular, a γ rhythm emerging from a fast interneuron loop modulates (and is modulated by) the internal slower rhythm emerging from the other loops. Finally, the last model (named the "coupled complete model") was obtained by considering the interaction between two or three interconnected ROIs; it can simulate more complex multimodal spectra, with a variety of rhythms (some intrinsic and some received from other ROIs) similar to those observed in vivo. In particular, the results stress that long-range excitatory synapses with time delay, directed to fast interneurons are particularly effective in transmitting rhythms from one region to another. These results, which may be tested by ad hoc experiments, can help the construction of more adequate models to fit in vivo data, and can be exploited to attain a deeper comprehension of the effect of connectivity patterns among ROIs.

References

Achard, S., Bullmore, E., 2007. Efficiency and cost of economical brain functional networks. PLoS Comput. Biol. 3, e17.

Babajani, A., Soltanian-Zadeh, H., 2006. Integrated MEG/EEG and fMRI model based on neural masses. IEEE Trans. Biomed. Eng. 53, 1794–1801.

Bartos, M., Vida, I., Jonas, P., 2007. Synaptic mechanisms of synchronized gamma oscillations in inhibitory interneuron networks. Nat. Rev. Neurosci. 8, 45–56.

Basar, E., Basar-Eroglu, C., Karakas, S., Schurmann, M., 2000. Brain oscillations in perception and memory. Int. J. Psychophysiol. 35, 95–124.

Basar, E., Basar-Eroglu, C., Karakas, S., Schurmann, M., 2001. Gamma, alpha, delta, and theta oscillations govern cognitive processes. Int. J. Psychophysiol. 39, 241–248.

Buzsàki, G., 2006. Rhythms of the Brain. Oxford University Press, New York.

Cobb, S.R., Buhl, E.H., Halasy, K., Paulsen, O., Somogyi, P., 1995. Synchronization of neuronal activity in hippocampus by individual GABAergic interneurons. Nature 378, 75–78.

Cobb, S.R., Halasy, K., Vida, I., Nyiri, G., Tamas, G., Buhl, E.H., Somogyi, P., 1997. Synaptic effects of identified interneurons innervating both interneurons and pyramidal cells in the rat hippocampus. Neuroscience 79, 629–648.

Cona, F., Zavaglia, M., Astolfi, L., Babiloni, F., Ursino, M., 2009. Changes in EEG power spectral density and cortical connectivity in healthy and tetraplegic patients during a motor imagery task. Comput. Intell. Neurosci. 279515 –.

Cunningham, M.O., Davies, C.H., Buhl, E.H., Kopell, N., Whittington, M.A., 2003. Gamma oscillations induced by kainate receptor activation in the entorhinal cortex in vitro. J. Neurosci. 23, 9761–9769.

David, O., Friston, K.J., 2003. A neural mass model for MEG/EEG: coupling and neuronal dynamics. Neuroimage 20, 1743–1755.

David, O., Harrison, L., Friston, K.J., 2005. Modelling event-related responses in the brain. Neuroimage 25, 756–770.

Engel, A.K., Singer, W., 2001. Temporal binding and the neural correlates of sensory awareness. Trends Cogn. Sci. 5, 16–25.

Felleman, D.J., van Essen, D.C., 1991. Distributed hierarchical processing in the primate cerebral cortex. Cereb. Cortex 1, 1–47.

Freeman, W.J., 1975. Mass Action in the Nervous System. Academic Press, New York.

Freeman, W.J., 1978. Models of the dynamics of neural populations. Electroencephalogr. Clin. Neurophysiol. 34, 9–18.

Freund, T.F., Buzsaki, G., 1996. Interneurons of the hippocampus. Hippocampus 6, 347–470.

Friston, K.J., 2005. Models of brain function in neuroimaging. Annu. Rev. Psychol. 56, 57–87.

Gonzalez-Burgos, G., Krimer, L.S., Povysheva, N.V., Barrionuevo, G., Lewis, D.A., 2005. Functional properties of fast spiking interneurons and their synaptic connections with pyramidal cells in primate dorsolateral prefrontal cortex. J. Neurophysiol. 93, 942–953.

Grimbert, F., Faugeras, O., 2006. Bifurcation analysis of Jansen's neural mass model. Neural. Comput. 18, 3052–3068.

Gutfreund, Y., Yarom, Y., Segev, I., 1995. Subthreshold oscillations and resonant frequency in guinea-pig cortical neurons: physiology and modelling. J. Physiol. (Lond). 483 (Pt. 3), 621–640.

Jansen, B.H., Rit, V.G., 1995. Electroencephalogram and visual evoked potential generation in a mathematical model of coupled cortical columns. Biol. Cybern. 73, 357–366.

Jansen, B.H., Zouridakis, G., Brandt, M.E., 1993. A neurophysiologically-based mathematical model of flash visual evoked potentials. Biol. Cybern. 68, 275–283.

Jefferys, J.G., Traub, R.D., Whittington, M.A., 1996. Neuronal networks for induced '40 Hz' rhythms. Trends Neurosci. 19, 202–208.

Kiebel, S.J., Garrido, M.I., Moran, R.J., Friston, K.J., 2008. Dynamic causal modelling for EEG and MEG. Cogn. Neurodyn. 2, 121–136.

Kisvarday, Z.F., Beaulieu, C., Eysel, U.T., 1993. Network of GABAergic large basket cells in cat visual cortex (area 18): implication for lateral disinhibition. J. Comp. Neurol. 327, 398–415.

Llinas, R.R., Grace, A.A., Yarom, Y., 1991. In vitro neurons in mammalian cortical layer 4 exhibit intrinsic oscillatory activity in the 10- to 50-Hz frequency range. Proc. Natl. Acad. Sci. U. S. A. 88, 897–901.

Lopes da Silva, F.H., Hoeks, A., Smits, H., Zetterberg, L.H., 1974. Model of brain rhythmic activity. The alpha-rhythm of the thalamus. Kybernetik 15, 27–37.

Maex, R., De, S.E., 2007. Mechanism of spontaneous and self-sustained oscillations in networks connected through axo-axonal gap junctions. Eur. J. Neurosci. 25, 3347–3358.

Moran, R.J., Kiebel, S.J., Stephan, K.E., Reilly, R.B., Daunizeau, J., Friston, K.J., 2007. A neural mass model of spectral responses in electrophysiology. Neuroimage 37, 706–720.

Moran, R.J., Stephan, K.E., Kiebel, S.J., Rombach, N., O'Connor, W.T., Murphy, K.J., Reilly, R.B., Friston, K.J., 2008. Bayesian estimation of synaptic physiology from the spectral responses of neural masses. Neuroimage 42, 272–284.

Moran, R.J., Stephan, K.E., Seidenbecher, T., Pape, H.C., Dolan, R.J., Friston, K.J., 2009. Dynamic causal models of steady-state responses. Neuroimage 44, 796–811.

Neltner, L., Hansel, D., Mato, G., Meunier, C., 2000. Synchrony in heterogeneous networks of spiking neurons. Neural. Comput. 12, 1607–1641.

Nunez, P., 1995. Neocortical Dynamics and Human EEG Rhythms. Oxford University Press, New York.

Rennie, C.J., Wright, J.J., Robinson, P.A., 2000. Mechanisms of cortical electrical activity and emergence of gamma rhythm. J. Theor. Biol. 205, 17–35.

Rennie, C.J., Robinson, P.A., Wright, J.J., 2002. Unified neurophysical model of EEG spectra and evoked potentials. Biol. Cybern. 86, 457–471.

Robinson, P.A., Rennie, C.J., Wright, J.J., Bahramali, H., Gordon, E., Rowe, D.L., 2001. Prediction of electroencephalographic spectra from neurophysiology. Phys. Rev. E. Stat. Nonlin. Soft. Matter Phys. 63, 021903 –.

Rosanova, M., Casali, A., Bellina, V., Resta, F., Mariotti, M., Massimini, M., 2009. Natural frequencies of human corticothalamic circuits. J. Neurosci. 29, 7679–7685.

Rowe, D.L., Robinson, P.A., Rennie, C.J., 2004. Estimation of neurophysiological parameters from the waking EEG using a biophysical model of brain dynamics. J. Theor. Biol. 231, 413–433.

Sik, A., Penttonen, M., Ylinen, A., Buzsaki, G., 1995. Hippocampal CA1 interneurons: an in vivo intracellular labeling study. J. Neurosci. 15, 6651–6665.

Sotero, R.C., Trujillo-Barreto, N.J., Iturria-Medina, Y., Carbonell, F., Jimenez, J.C., 2007. Realistically coupled neural mass models can generate EEG rhythms. Neural Comput. 19, 478–512.

Thomson, A.M., West, D.C., Hahn, J., Deuchars, J., 1996. Single axon IPSPs elicited in pyramidal cells by three classes of interneurones in slices of rat neocortex. J. Physiol. 496 (Pt. 1), 81–102.

Tiesinga, P.H., Jose, J.V., 2000. Robust gamma oscillations in networks of inhibitory hippocampal interneurons. Network 11, 1–23.

Traub, R.D., Contreras, D., Cunningham, M.O., Murray, H., Lebeau, F.E., Roopun, A., Bibbig, A., Wilent, W.B., Higley, M.J., Whittington, M.A., 2005. Single-column

thalamocortical network model exhibiting gamma oscillations, sleep spindles, and epileptogenic bursts. J. Neurophysiol. 93, 2194–2232.
Ursino, M., Zavaglia, M., Astolfi, L., Babiloni, F., 2007. Use of a neural mass model for the analysis of effective connectivity among cortical regions based on high resolution EEG recordings. Biol. Cybern. 96, 351–365.
Wang, X.J., Buzsaki, G., 1996. Gamma oscillation by synaptic inhibition in a hippocampal interneuronal network model. J. Neurosci. 16, 6402–6413.
Ward, L.M., 2003. Synchronous neural oscillations and cognitive processes. Trends Cogn. Sci. 7, 553–559.
Wendling, F., Bartolomei, F., Bellanger, J.J., Chauvel, P., 2002. Epileptic fast activity can be explained by a model of impaired GABAergic dendritic inhibition. Eur. J. Neurosci. 15, 1499–1508.
White, J.A., Chow, C.C., Ritt, J., Soto-Trevino, C., Kopell, N., 1998. Synchronization and oscillatory dynamics in heterogeneous, mutually inhibited neurons. J. Comput. Neurosci. 5, 5–16.
White, J.A., Banks, M.I., Pearce, R.A., Kopell, N.J., 2000. Networks of interneurons with fast and slow gamma-aminobutyric acid type A (GABAA) kinetics provide substrate for mixed gamma-theta rhythm. Proc. Natl. Acad. Sci. U. S. A. 97, 8128–8133.
Whittington, M.A., Traub, R.D., Jefferys, J.G., 1995. Synchronized oscillations in interneuron networks driven by metabotropic glutamate receptor activation. Nature 373, 612–615.
Wilson, H.R., Cowan, J.D., 1972. Excitatory and inhibitory interactions in localized populations of model neurons. Biophys. J. 12, 1–24.
Wright, J.J., Rennie, C.J., Lees, G.J., Robinson, P.A., Bourke, P.D., Chapman, C.L., Gordon, E., Rowe, D.L., 2003. Simulated electrocortical activity at microscopic, mesoscopic, and global scales. Neuropsychopharmacology 28 (Suppl. 1), S80–S93.
Zavaglia, M., Astolfi, L., Babiloni, F., Ursino, M., 2006. A neural mass model for the simulation of cortical activity estimated from high resolution EEG during cognitive or motor tasks. J. Neurosci. Methods 157, 317–329.
Zavaglia, M., Astolfi, L., Babiloni, F., Ursino, M., 2008. The effect of connectivity on EEG rhythms, power spectral density and coherence among coupled neural populations: analysis with a neural mass model. IEEE Trans. Biomed. Eng. 55, 69–77.